Biotribology 17 (2019) 64–74

Contents lists available at ScienceDirect

Biotribology

journal homepage: www.elsevier.com/locate/biotri

The Dynamic Friction Coefficient of the Wet Bone-Implant Interface: Influence of Load, Speed, Material and Surface Finish

Charlotte Voutat[a], Jiri Nohava[b,*], Jasmin Wandel[c], Philippe Zysset[a]

[a] ARTORG Centre for Biomedical Engineering Research, University of Bern, Bern, Switzerland
[b] Anton Paar Tritec SA, Peseux, Switzerland
[c] Institute for Risks and Extremes, Bern University of Applied Sciences, Burgdorf, Switzerland

ARTICLE INFO

Keywords:
Bone
Implant
Friction

1. Introduction

Joint replacement by prosthetic implants such as hip arthroplasty or dental implantation represents today an important part of medical care mainly due to ageing of our populations [1]. While the surgical techniques are well mastered nowadays, there are still unknown processes that might slow down the process of healing. Primary mechanical stability of the bone-implant interface is one of the factors that strongly affects the osseointegration necessary for fast healing and long term stability of the implant. Indeed, if the implant subjected to daily loading exhibits excessive micromotions with respect to the bone, its osseointegration is slowed down or completely arrested which can lead to the formation of a fibrous tissue layer, pain and eventual loosening of the implant [2–4]. The phenomenon of implant-bone micromotions has been studied for more than two decades both experimentally and by computer modeling. However, the knowledge on the contact mechanics between bone and various implant surfaces is still limited and various results were obtained by different authors [5–7] (see Fig. 1 and Table 1). Especially in cortical bone, frictional forces depend critically on the extent of damage produced by insertion of the implant and these effects therefore need to be investigated independently in more detail. Moreover, the frictional behavior may involve a third body when substantial wear between implant parts or between implant and bone is produced. For uncemented hip implants, it has been shown that micromotions at bone implant-interface in the range of 100 μm occur when physiological loads are applied, for example during gait [4,8]. These micro-motions (which cannot be completely eliminated) should be minimized to allow for fast healing process and proper osseointegration. The micromotions will depend on the coefficient of friction (CoF), which is strongly related to the material and state of the surface of the implants. These are usually manufactured from stainless steel (316 L), titanium or titanium alloys and often have some specific surface treatment to promote bone ingrowth. The state of the surface of the implant and its effect on the friction should therefore also be investigated. Table 1 summarizes some of the studies of frictional properties between bone and implant. Generally, the CoF was obtained using flat-on-flat tribological tests with various loads. In most of the studies, sliding speed and/or load was kept constant. The CoF was found to vary greatly (sometimes even within a single study) and it would be almost impossible to use these results for an assessment of stability of a new implant design using numerical simulation. Well founded numerical study of implant stability requires indeed an extension of the range of parameters tested, both in load and speed but also in materials and their surface treatments.

The aim of this work was to study the frictional properties of selected bone-implant pairs in linear reciprocal movements under various contact conditions. Stainless steel, titanium alloy and commercially pure titanium were used to model the implant material and they were tested against cortical bone samples extracted from bovine tibia. The tribological experiments were done at various speeds and loads so that the influence of sliding speed and load on the coefficient of friction could be determined. The outcomes of this work shall contribute to the understanding of the frictional properties between implant and bone in the first weeks post-operation and will help in further modeling of the bone-implant contact.

* Corresponding author.
E-mail address: jiri.nohava@anton-paar.com (J. Nohava).

https://doi.org/10.1016/j.biotri.2019.03.002
Received 19 November 2018; Received in revised form 21 February 2019; Accepted 1 March 2019
Available online 03 March 2019

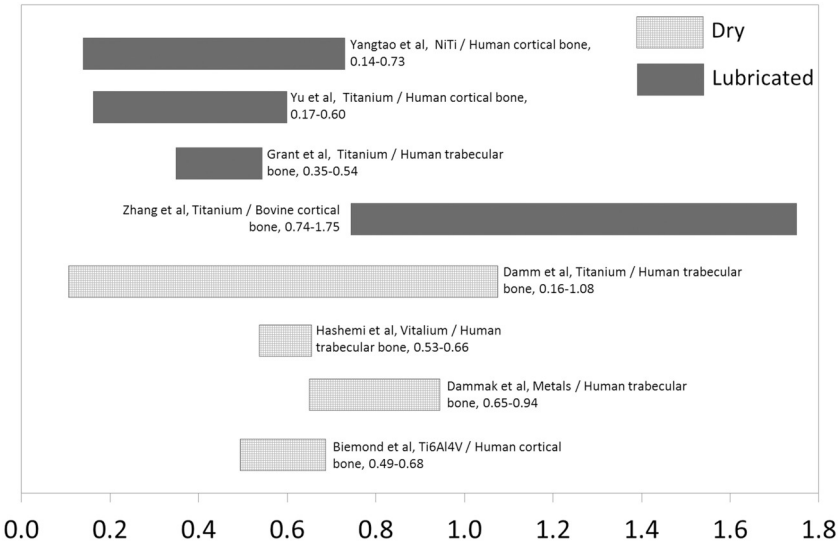

Fig. 1. Coefficient of friction as measured by different authors under various conditions. For more details see Table 1.

2. Materials and Methods

2.1. Bone Samples

Cortical bone samples were extracted from healthy bovine tibiae obtained from a local butchery. The samples were cut into cylinders of ~40 mm height and the bone marrow was removed. The remaining hollow cylinders were then cut in the axial direction into ~20 mm wide blocks. The outer surface of these blocks was glued to an aluminum support using two-component epoxy glue to ensure solid attachment of the bone to the support while the inner surface was milled with a microtome. After milling, the surface was polished first with sand paper and then using diamond polishing paste. To remove the remaining debris, samples were cleaned for 15 min in an ultrasonic bath. All samples were fresh-frozen and immersed in saline solution before testing.

2.2. Implant Materials

Stainless steel (316 L), Ti6Al7Nb alloy and commercially pure Titanium (CP Ti) (all with surface finish corresponding to clinical use) pins with a spherical end of 10 mm radius were used as implant models. These materials are commonly used for hip prostheses or dental implants. In order to study the effect of surface finish, the CP Ti pin was also manufactured with a sand blasted surface and with a surface treatment which was obtained by anodization. This surface treatment resulted in partially crystalline structure and phosphate enriched titanium oxide characterized by a micro-structured surface with open pores in the low micrometer range (denoted here as 'surface treatment'). All these surface finishes were applied to the spherical part of the pin that was in contact with the bone. The elastic moduli of the implant materials and the roughness of the surfaces are given in Table 2, while representative images of the three surface finishes (polishing, sand blasting and surface treatment) are shown in Fig. 2. The elastic modulus values were provided by the manufacturer whereas the surface roughness was measured using a mechanical profilometer (Taylor Hobson, Leicester, UK). Since negligible wear of the pins was observed, the pins were reused for experiments with different speeds. However, a new pin was used for each level of load.

2.3. Frictional Parameter Considerations

The yield stress of bovine cortical bone in the radial direction in tension is approximately 76 MPa and the corresponding value in compression is 113 MPa [17]. The contact pressure used in our experiments were selected in order to study the frictional properties of the bone in the elastic regime (< 113 MPa), in the transition regime between elastic and plastic regime (~113 MPa) and above the yield stress (> 113 MPa). The levels of load used in our experiments together with the maximum Hertzian pressure are given in Table 3. The minimal load applied on the contacting sphere of the metal pin was chosen so that it exceeded the typical pressure of a press-fitted implant as calculated according to press-fit pressure formulae in [18] (~30 MPa).

Another important factor in contact mechanics is the sliding speed. For the tribological tests to be relevant to the real locomotion, the sliding velocity should be related to the speed of micro-motions experienced during gait. This speed is given by the extent of the micromotion (100 μm) and the frequency of walking (approximately one step per second). The average speed of the micromotions during walking is therefore ~100 μm/s. However, sudden rapid movements of the implant versus bone (such as jumps) are also expected and therefore frictional properties at higher sliding speeds should be investigated.

The effects of friction are especially important during the primary stability phase, i.e. several weeks after the implantation of the prosthesis. After this period, the stability of the implant is determined more by the osseointegration and bone ingrowth and the frictional properties are less important than during the primary stabilization phase. The duration and the total sliding distance of the test should therefore simulate this period. However, simulation over a period of several weeks is generally extremely difficult to realize. Therefore, an accelerated test protocol related to the distance of movement during the primary stability period was defined. This distance $\boldsymbol{d}$ is calculated according to

$$d = d_s nt \tag{1}$$

where $\boldsymbol{d_s}$ is the total micromotion distance during gait (2 × 100 μm), $\boldsymbol{n}$ is number of steps during a day (~6′000) and $\boldsymbol{t}$ is the primary stability period (~6 weeks, i.e. 42 days). Using these values in (1) gives a total test distance of 50.4 m. The duration of one tribological test is determined as the distance $\boldsymbol{d}$ divided by the sliding speed. This results in test duration of approximately 14 min for the highest sliding speed (94×10^3 μm/s) and tribometer cycle length of 60 mm. This duration of experiment was kept also for lower sliding speeds but the tribometer cycle length was decreased to 3 mm in order to achieve the lowest sliding speeds.

Table 1
Summary of recent studies on friction at the bone implant interface. Materials, test conditions and results are listed for each study.

Author	Materials tested	Test conditions	Lubricant	Friction coefficient
Biemond et al. [9]	Human cortical bone Ti-6Al-4 V with different surface treatments	Flat-on-flat 0.33 mm/s over 30 mm Normal force: 40 N Surface in contact: 7 × 20 mm^2	No	0.49–0.68
Zhang et al. [10]	Bovine cortical and cancellous bone Porous tantalum with different topographies	Flat-on-flat Normal force: 4.4 N + weight of samples Surface in contact: 400 mm^2 Static friction coefficient: angle of slippage	Wetted with saline	Cortical bone: 0.74–1.75 Cancellous bone: 0.88–0.98
Dammak et al. [11]	Human trabecular bone Different types of metallic surfaces	Flat-on-flat Pressure: 0.10 MPa and 0.25 MPa	No	0.65–0.94
Hashemi et al. [12]	Human trabecular bone Vitallium bead porous-coated plate	Flat-on-flat (bidirectional) Pressure: 0.1 MPa	No	0.53–0.66
Damm et al. [13]	Human trabecular bone Polished, beaded and flaked titanium platens	Flat-on-flat (push-in/pull-out) Pressure: 0–12 MPa	No	Polished: 0.16 Beaded: 0.86 Flaked: 1.08
Grant et al. [14]	Artificial and human trabecular bone Titanium with different surface treatments	Flat-on-flat Pressure: 0.25–1 MPa Speed: ~ 4 mm/s	Bovine fetal serum	Artificial: 0.36–0.56 Human: 0.35–0.54
Yu et al. [15]	Human cortical bone Titanium and Titanium alloy	Ball-on-flat Normal load: 25–98 N Displacement: 3–45 µm Frequency: 2 Hz	Imitated human physiological solution	Titanium: 0.17–0.60 Titanium alloy: 0.29–0.65
Yangtao et al. [16]	Human cortical bone Nickel-Titanium shape memory alloy	Cylinder-on-flat Normal load: 100 N Displacement: 70–300 µm Frequency: 5 Hz Cylinder size: ∅15 × 22 mm	No Hank's solutions	0.14–0.73

Table 2
List of pin materials, their mechanical properties and surface finish.

Material	Elastic modulus E	Surface finish	Surface roughness R_a
CP Ti	105 GPa	Polished	0.14 µm
		Surface treatment	0.90 µm
		Sand blasted	0.29 µm
Ti6Al7Nb alloy	105 GPa	Polished	0.14 µm
Stainless steel 316 L	200 GPa	Polished	0.15 µm

2.4. Tribological Experiments

The tribological experiments were done using a pin-on-disk tribometer (Tribometer, Anton Paar, Switzerland) at various loads and linear speeds with the sample and the metallic pin completely immersed in saline solution (0.9% NaCl in water) at room temperature (24 °C). All tribological experiments were done in linear reciprocating mode to simulate the sliding movements of the implant versus bone (Fig. 3). Five levels of forces (Table 3) were applied in order to test both elastic and plastic deformation regimes: two levels of forces in the reversible regime (1 N and 3 N), two in the irreversible regime (30 N and 50 N) and one in the transition regime (8 N). The sliding speeds selected were 94 µm/s, 94×10^1 µm/s, 94×10^2 µm/s and 94×10^3 µm/s so that a broad range of real life conditions (from normal gait movements at ~94 µm/s up to jumps at 94×10^3 µm/s) could be simulated. All experiments were done with the spherical end of the metallic pin in contact with the bone. In most of the experiments the pin was sliding along the axial direction of the bone; however a series of experiments was done also with the sliding movement in the radial direction (perpendicular to the axis of the bone). Since the sliding speed is goniometric function of position in linear reciprocating movement, only the CoF values acquired between −5 mm and + 5 mm and between −0.5 mm and + 0.5 mm from the center of the 30 mm and the 3 mm long cycle respectively were used. In this range the sliding speed varied between 94% and 100% of the maximum speed.

The tribological tests aimed to study combinations of these effects:

- Vertical load and speed effects: a total of one hundred tests with stainless steel 316 L were realized: five repetitions for each combination of load (Table 3) and speed. All tests were conducted along the axial direction (parallel to fiber direction). For each test a new bone sample was used.
- Material and speed effects: a total of one hundred tests were performed for each combination of material and speed (five repetitions for each combination) at the load of 8 N, in the axial direction. A new bone sample for each test was used.
- Direction and speed effects: a total of 40 tests were performed for each combination of direction and speed (five repetitions for each combination) using 316 L steel and 8 N load.

2.5. Analysis of the Results

The results of the tribological tests were evaluated both by descriptive statistics and exploratory statistics. To be able to account for the dependency among the repeated measures, multiple linear random-effects models were used to estimate the effects of the test parameters (speed, load, material and sliding direction) on the coefficient of friction. Further, a logarithmic transformation of all explanatory variables was used in order to meet the model assumptions. Specifically, the following models were implemented:

- load, speed with interaction

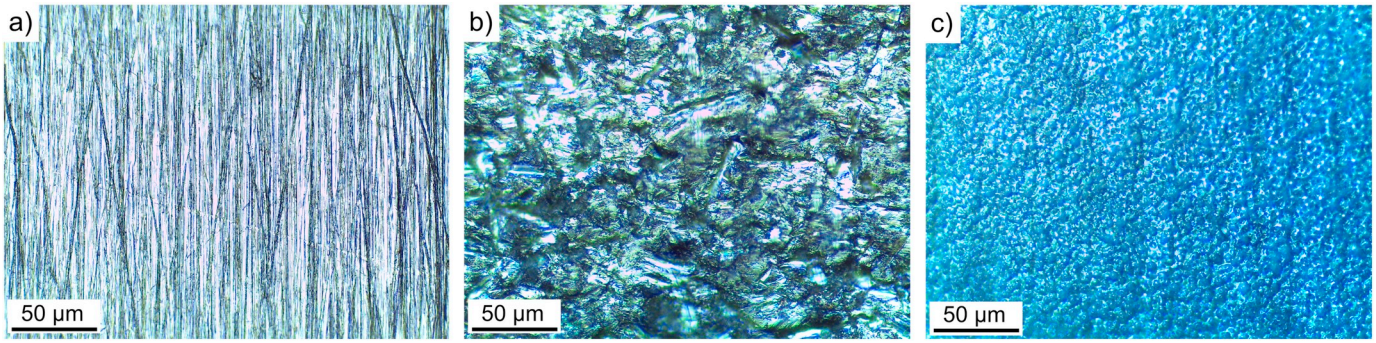

Fig. 2. Optical microscopy images of the three types of surface treatment: 1) polished, b) sand blasted and c) surface treatment.

Table 3
Maximum Hertzian pressure in bone (using E = 10 GPa and v = 0.45 for bone).

Load [N]	Maximum Hertzian contact pressure against steel [MPa]
1	~60
3	~90
8	~130
30	~200
50	~240

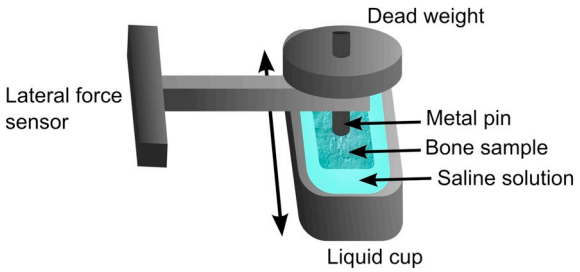

Fig. 3. Schematic illustration of the linear reciprocating tribological experiment.

$$\mu_{ij}(P,v) = A_1 + A_2\log(P_{ij}) + A_3\log(v_{ij}) + A_4\log(P_{ij})\log(v_{ij}) + U_i + \varepsilon_{ij} \quad (2)$$

– material and speed

$$\mu_{ij}(v) = B_1 + B_2\log(v)_{ij} + U_i + \varepsilon_{ij} \quad (3)$$

– sliding direction and speed

$$\mu_{ij}(v) = C_1 + C_2\log(v)_{ij} + U_i + \varepsilon_{ij} \quad (4)$$

μ denotes the coefficient of friction, P the applied load and v the sliding speed. Further, U_i denotes the random effect for each repetition (i = 1,2,3,4,5) and ε_{ij} the individual random error terms. Likelihood ratio tests were used to calculate the p-values for the fixed effects in the described models, as well as for the comparisons of different models. No adjustment for multiple testing was performed. As random-effects models were used, two values of R^2 were evaluated for each model:

– Marginal R^2: describes the proportion of variance explained by fixed effects solely,
– Conditional R^2: describes the proportion of variance explained by both fixed and random effects.

Plots with the fitted model were also generated and two types of intervals were added to these plots:

– The 95% confidence intervals, giving an impression about the goodness of fit,
– The 95% prediction interval (estimated via bootstrap), indicating the area where a future data point would lie (with 95% certainty).

3. Results

3.1. Vertical Load and Speed Effects

Fig. 4 shows the coefficient of friction as a function of sliding speed and applied load for the polished 316 L stainless steel. On average, for 1 N load, the coefficient of friction decreases with increasing sliding speed from a value of ~0.6 to a value of ~0.2. A similar decrease of the CoF with increasing sliding speed was observed for each of the applied loads (1 N, 3 N, 8 N, 30 N and 50 N). A comparison of CoF at constant speed (for example 94 µm/s) for all applied loads shows that the CoF for given speed is decreasing with increasing load. This decrease of the CoF was most pronounced for the lowest sliding speed (94 µm/s) whereas it was less pronounced at higher sliding speeds. At the highest sliding speed (94×10^2 µm/s and 94×10^3 µm/s) the CoF remained roughly constant for all applied loads. A closer look at the lowest sliding speeds indicates that the CoF seems to reach a plateau with value of 0.6 for 1 N load, 0.5. for 3 N, 0.45 for 8 N and 0.4 for 30 N and 50 N.

The random-effects model shows that the effect of load on CoF is statistically significant ($p < 0.05$), i.e. the slope of the fit is different for each load (see Fig. 5 and Table 4). The effects of speed, as well as the interaction between speed and load are statistically significant as well ($p < 0.05$). Overall, the 95% confidence interval for the average coefficient of friction is $\mu \pm 0.13$, the marginal R^2 is 0.65 and the conditional R^2 is 0.77.

3.2. Material, Surface Finish and Speed Effects

The influence of material and its surface finish on the CoF is shown in Fig. 6. All the tests were performed with a load of 8 N. The 316 L, pure Ti and Ti6Al7Nb alloy samples had polished surface whereas "sand blasted" and "Surface treatment" was applied to the CP Ti samples. For all tested materials the CoF decreased with increasing speed; however there seemed to be a plateau with constant CoF for the lowest sliding speeds. On average, the CoF value was ~0.4 for the 316 L steel and ~0.6 for all the other materials except the CP Ti with Surface treatment where the plateau was less pronounced. The polished 316 L steel exhibited the lowest CoF out of all materials and surfaces tested.

The results of the random-effects model are shown in Fig. 7 and Table 5. Again, Fig. 7 shows the means of five repetitions per test, the model fit, the 95% confidence interval and the 95% prediction interval. The estimated parameters of each model (Eq. (3)) are the diagonal (bold) values in Table 5: the first parameter is indicating the intercept of the fit (i.e. CoF for the speed of 1 µm/s on logarithmic scale) and the second parameter the slope of the fit. For example, commercially pure titanium has parameter B_1 (intercept) 7.97×10^{-1} and parameter B_2 (slope) -3.64×10^{-2}.

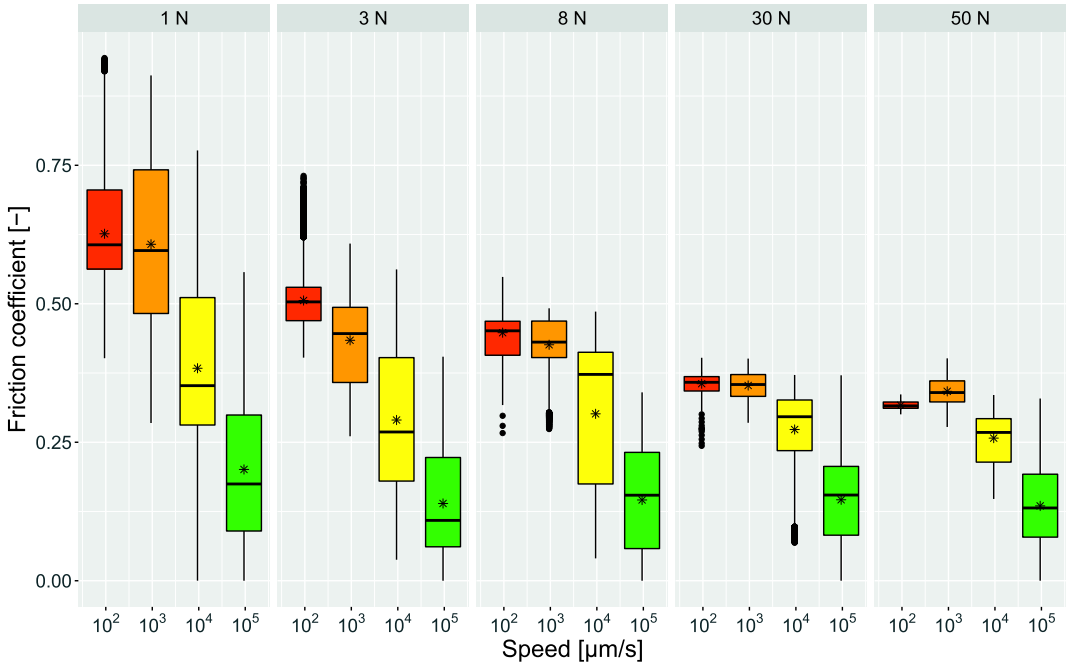

Fig. 4. Friction coefficient as a function of speed and applied load on the 316 L.

The off-diagonal, non-bold values, estimate the differences in intercept and slope between the given materials. For example, the intersection of Ti6Al7Nb alloy column and CP Ti row can be interpreted in the following manner: the estimated intercept for Ti6Al7Nb is 3.65×10^{-2} larger (p-value > 0.05) and the slope 3.34×10^{-3} smaller (p-value < 0.05) than for CP Ti. Therefore, the slopes of these two fits are different with 95% certainty. A difference in the slope means that for the same speed variation, the coefficients of friction do not vary in the same way. Since all slope parameters are significantly different, it means that the CoF of all materials (and surface treatments) vary differently with speed. On the other hand, a difference in the

Table 4
Estimated parameters of random-effects model for load and speed effects.

Variable	Coefficient
Intercept (A_1)	9.416×10^{-1}*
Log(load) (A_2)	-1.233×10^{-1}*
Log(speed) (A_3)	-6.429×10^{-2}*
Log(load)*log(speed) (A_4)	9.620×10^{-3}*

* $p < 0.05$

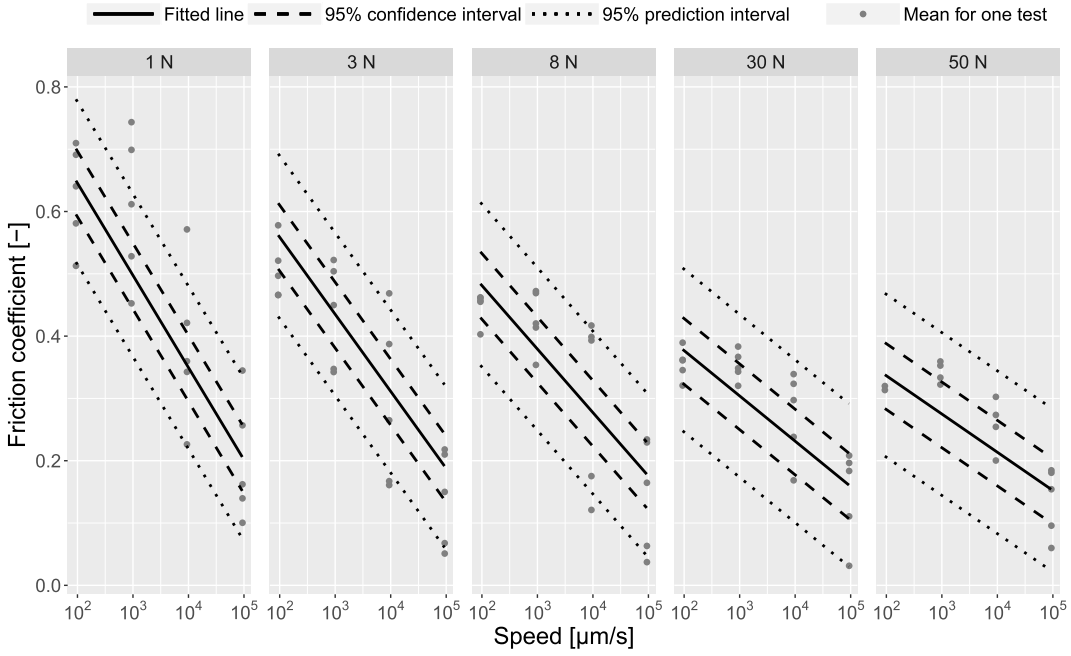

Fig. 5. Random-effects model for the effect of speed and load on CoF for 316 L steel showing the fit, confidence interval and prediction interval for each applied load.

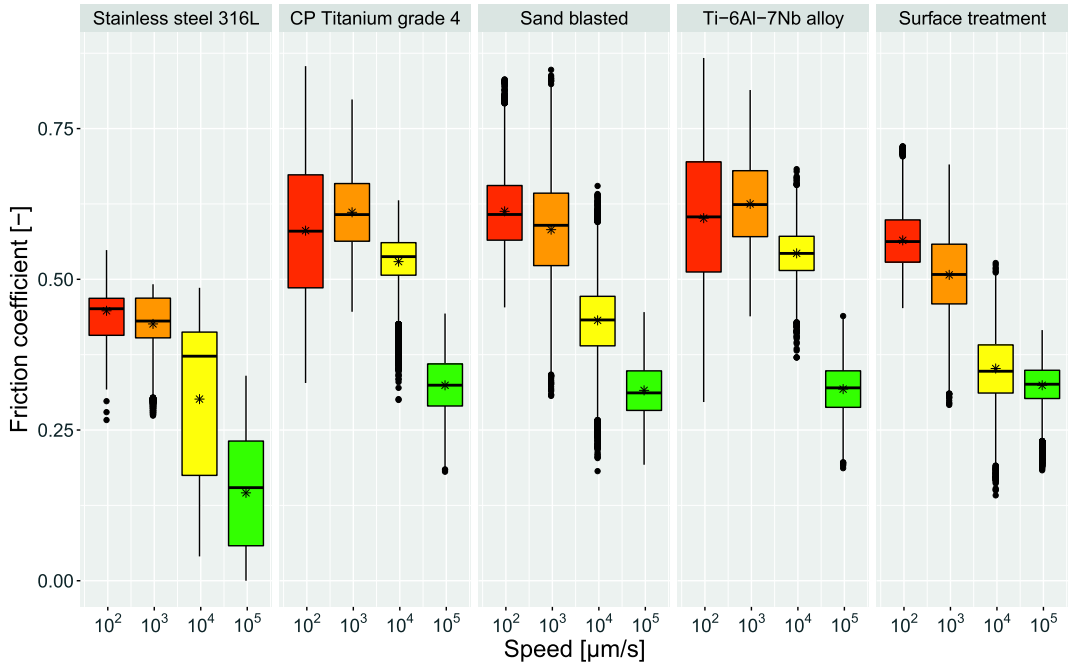

Fig. 6. Friction coefficient as a function of sliding speed, implant material and surface finish (the Sand blasted and Surface treatment modifications were applied to the CP Ti sample only).

intercept means that the estimated friction coefficient is not the same at 1 µm/s. The intercept for stainless steel 316 L is significantly different from the other materials (except for the CP Ti with surface treatment). There is no significant difference between intercepts for CP Ti, Ti-Al-7Nb alloy and sandblasted CP Ti. Overall, the marginal R^2 is 0.69 and the conditional R^2 0.76. The 95% confidence interval for the average coefficient of friction is $\mu \pm 0.084$.

3.3. Effect of Sliding Direction (Circumferential Versus Axial)

Fig. 8 shows a comparison of the CoF of sliding in circumferential (perpendicular to fibers) and axial (parallel to fibers) directions at various sliding speeds. The data were obtained using the 316 L steel pin and 8 N load. On average, the coefficient of friction decreases with increasing sliding speed for both sliding directions – except for the lowest sliding speeds where the CoF seems to reach a plateau of ~0.45 for both sliding directions at the lowest speeds. The CoF at higher speeds is higher for the circumferential direction (perpendicular to the fibers) than for the axial direction.

A random-effects model according to Eq. (4) was applied in this case (Fig. 9). Table 6 shows the estimated parameters of the fit to the experimental data; the interpretation of the results in the diagonal and off-diagonal cells is analogical to that of cells in Table 5. The non-significant difference (no asterisk) between the estimated intercepts means

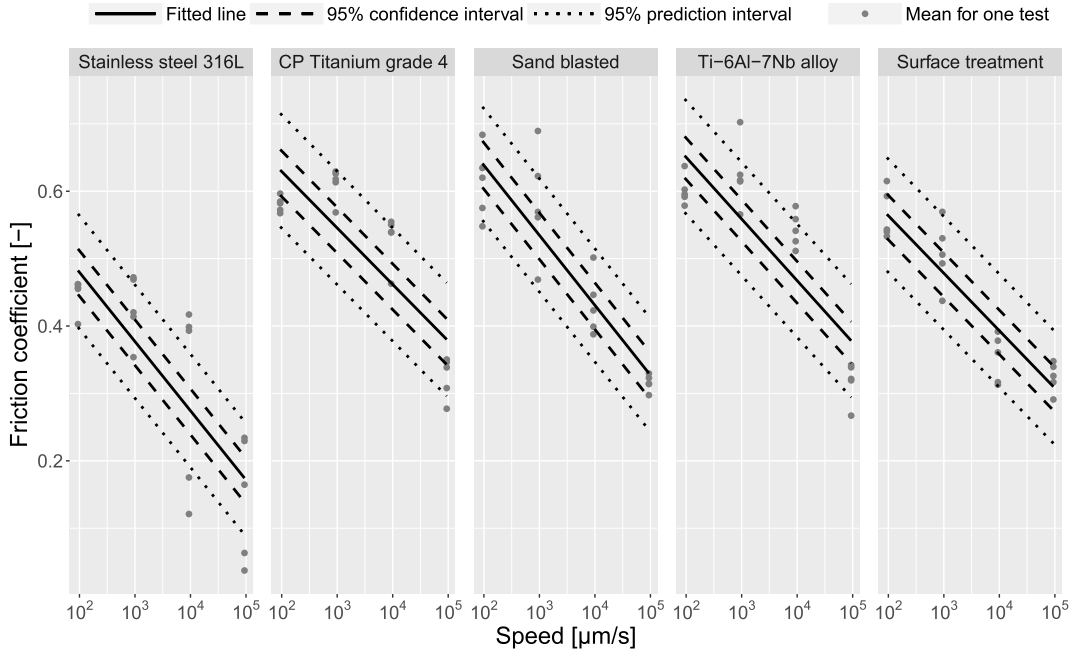

Fig. 7. Random-effects model fit of speed, material and surface finish.

Table 5
Estimated parameters of the random-effects model (B_1 and B_2) for different implant materials and surface finish. The diagonal values are the parameters of the Eq. (3) fit and the off-diagonal values are the differences between the fit parameters for the given combination of materials (* $p < 0.05$).

	Stainless steel 316L	CP Ti	CP Ti (sand blasted)	Ti6Al7Nb	CP Ti (surface treatment)
Stainless steel 316L	**6.85×10^{-1}*** **-4.46×10^{-2}***	1.12×10^{-1}* 8.19×10^{-3}*	1.61×10^{-1}* -4.86×10^{-4}*	1.48×10^{-1}* 4.85×10^{-3}*	4.91×10^{-2} 7.55×10^{-3}*
CP Ti		**7.97×10^{-1}*** **-3.64×10^{-2}***	4.91×10^{-2} -8.68×10^{-3}*	3.65×10^{-2} -3.34×10^{-3}*	-6.28×10^{-2}* -6.38×10^{-4}*
CP Ti (sand blasted)			**8.46×10^{-1}*** **-4.51×10^{-2}***	-1.26×10^{-2} 5.33×10^{-3}*	-1.12×10^{-1}* 8.04×10^{-3}*
Ti6Al7Nb				**8.33×10^{-1}*** **-3.97×10^{-2}***	-9.92×10^{-2}* 2.71×10^{-3}*
CP Ti (surface treatment)					**7.34×10^{-1}*** **-3.70×10^{-2}***

* $p < 0.05$

that at low speed the friction coefficient is not significantly different for the two sliding directions. However, the estimated difference of the slopes is significant. The marginal R^2 is 0.65 and the conditional R^2 is 0.77. The 95% confidence interval for the average coefficient of friction is $\mu \pm 0.1$.

4. Discussion

The dynamic frictional properties of implant versus bone were studied under different conditions (load, sliding speed, material, surface finish and sliding direction) in order to obtain relevant data for further optimization and modeling of implant-bone interface. While the lower speeds simulated steady (walking) conditions, the higher speeds simulated situations when the implant is subjected to sudden and rapid motions (jumps). The range of loads was selected in order to simulate both natural conditions and higher pressures occurring during momentarily overloading. Use of different materials and surface finishing of CP Ti should help in elucidating their effects on the coefficient of friction between the bone and implant. Finally, orthogonal sliding directions were investigated to check the influence of the bone microstructure.

4.1. Effects of Load and Sliding Speed

The observed decrease of CoF with increasing load is very likely related to local conditions at the surface: at higher loads, the surface asperities of the bone (although polished) are further flattened by plastic deformation, thus making the surface flatter, which results in lower resistance to sliding and hence lower CoF. Similar trend was observed also by Chowdhury [19] who however explained this decrease of CoF by increased quantity of wear debris at higher loads, leading to easier sliding of the implant and thus lower CoF. Most likely, these two effects were combined and they were more pronounced at higher loads where larger deformations are expected. At the same time, variation in load affects the fluid flow at the interface between the surface of the bone and the surface of the implant, which contributes significantly to the lubrication. The combined effect of load and speed in lubricated sliding contact can be described by the Stribeck curve [20], where the CoF is plotted as a function of Hersey's number, which is defined as $v \times \eta/P$ where v is sliding speed, η is viscosity and P is load. The CoF from our experiments as a function of Hersey's number is shown in Fig. 10. This chart can be considered in two ways: CoF as a function of speed and CoF as a function of load. While the influence of speed (at

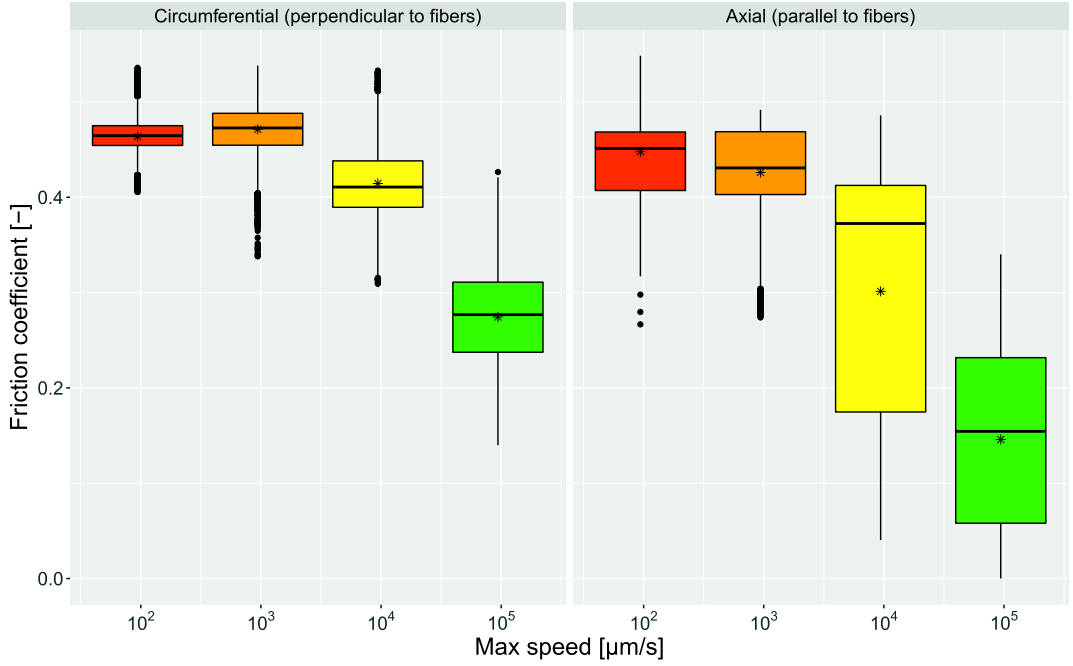

Fig. 8. Influence of the sliding direction on the coefficient of friction.

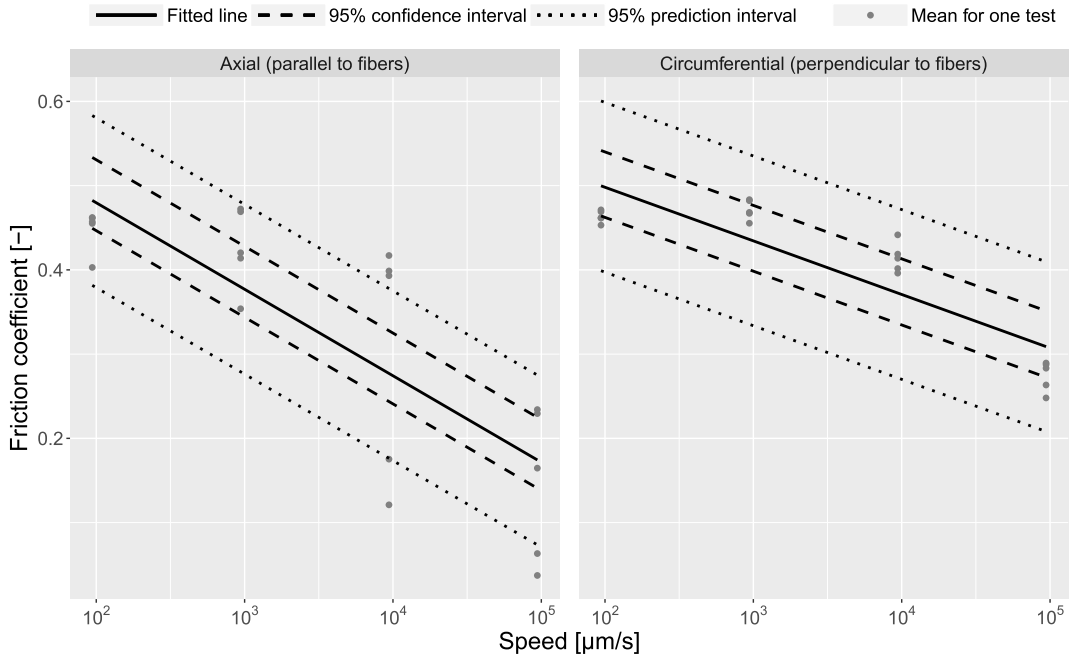

Fig. 9. Random-effects model fit of speed and sliding orientation on CoF.

Table 6
Estimated parameters of the random-effects model (C_1 and C_2) for speed and sliding direction.

	Axial	Circumferential
Axial	$\mathbf{6.85 \times 10^{-1}}_*$ $\mathbf{-4.46 \times 10^{-2}}_*$	-5.97×10^{-2} $1.70 \times 10^{-2}_*$
Circumferential		$\mathbf{6.25 \times 10^{-1}}_*$ $\mathbf{-2.76 \times 10^{-2}}_*$

* $p < 0.05$

constant load) indicates a plausible mixed lubrication (decrease of CoF with increasing Hersey's number), the influence of load (at constant speed) indicates rather hydrodynamic lubrication (increase of CoF with increasing Hersey's number), which is not credible at low speeds. The characterization of the lubrication regime with the Stribeck curve is therefore not adequate for the present experiment. However, one can note that the effect of load on CoF is much stronger than the effect of speed: the estimated slope of the logarithmic fit to CoF at constant speed (with varying load) is higher than the estimated slope with constant load (with varying speed) (see Table 4 and data in Appendix). In other words, variation of load by a factor of fifty (1 N to 50 N) results approximately in a two-fold decrease of the CoF whereas for the same increase (two- to three-fold) of the CoF the speed would have to vary by a factor of thousand. At load levels most relevant for the real application (i.e. low speeds and loads of 3 N to 8 N corresponding to walking), on average the CoF for the 316 L steel takes on a value of ~0.45. The strong effect of load is mostly pronounced at lower speeds whereas it tends to be less important at higher speeds. This effect shall be interpreted in respect to the increasing inelastic deformation of the bone with increasing load which reduces asperities and favors boundary lubrication.

The mean value of CoF at low speeds (~0.45) gives relevant information about the frictional behavior of bone and implant in the most

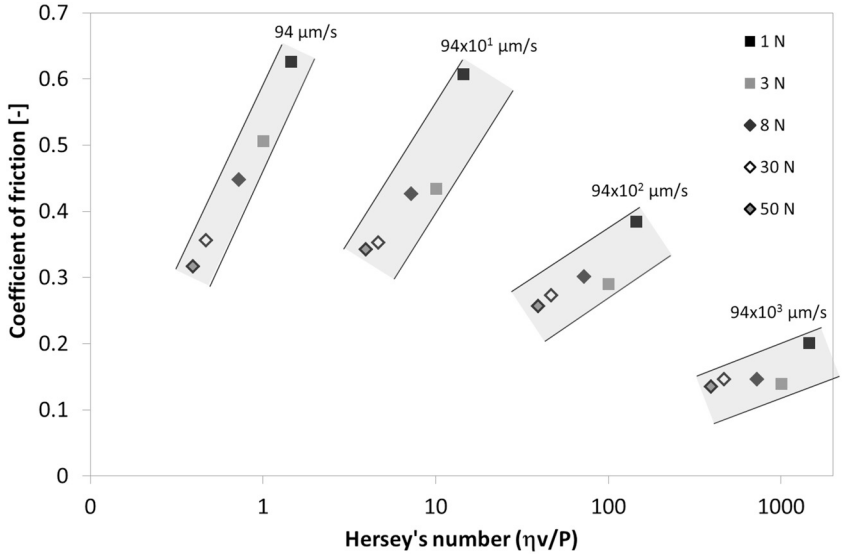

Fig. 10. CoF as a function of Hersey's number (speed ∗ viscosity/load).

often encountered condition (walking) during the primary stabilization phase. The value of CoF of 0.45for the 316 L steel and ~0.6 for the Ti and Ti alloys is also in good agreement with literature [21,22] and can thus be used in bone-implant models. It has to be mentioned that the measurements at 30 N and 50 N induced inelastic deformation in the bone. Although less relevant to the real life situation, these measurements were nevertheless important to determine the evolution of CoF at higher loads which can occasionally occur. It is a comforting outcome that at normal load conditions (i.e. below ~10 N) the coefficient of friction is higher than at higher load and thus favors the implant integration by reducing the micro-motions.

4.2. Effects of Material and Surface Finish

Similarly, as for the load and speed variation on the 316 L steel, the CoF decreases with increasing sliding speed on all tested materials and surface finish (Fig. 6). The CoF of 316 L steel is however considerably lower than the CoF of the other tested materials (CP Ti, Ti6Al7Nb alloy, CP Ti sand blasted and CP Ti with Surface treatment). The four other materials exhibit very similar CoF at corresponding sliding speeds, which indicates that the effect of material and surface finish on the CoF within this group is negligible. A general increase of CoF with increased surface roughness (CP Ti sand blasted and CP Ti with Surface treatment) was observed by Wang et al. [17]. Wang et al. studied the influence of surface roughness on CoF of tilt pad thrust bearings and found that the average lubricating film thickness increased with increasing surface roughness. In our case, given the large difference in hardness of the contacting materials, higher CoF can also be attributed to the ploughing effect of the CP Ti materials with additional surface treatment. Indeed, the asperities of the rougher CP Ti surfaces were in direct contact with the bone, which resulted in higher CoF. The descriptive statistics also showed that on average the value of CoF at 8 N and 94 μm/s is ~0.45 for 316 L steel and ~0.6 for CP Ti and Ti alloys. The increased CoF of Ti and Ti alloys seems to be due to the fact that these materials are more compliant than steel and deform more under the same load, which leads to increased contact area and hence larger CoF. It is therefore expected that implants from Ti and Ti alloys will have smaller displacements during the normal (walking) activity in the course of the post-operation stabilization period and hence heal more rapidly. The value of CoF for Ti and Ti alloy allows also for adapted input for modeling of titanium implants.

4.3. Effect of Sliding Direction

The effect of sliding direction was tested using 316 L steel material at load of 8 N at various speeds. Interestingly, there was no significant difference in CoF between sliding in the axial and circumferential direction at low speeds. At higher speeds however, the CoF was larger when sliding in the circumferential direction (i.e. perpendicular to the fiber direction) than when sliding in the axial direction (parallel to the fiber direction). This resembles the above mentioned effect of surface finish: the rougher surface (sliding direction perpendicular to the fibers) exhibited higher CoF than the smoother surface (sliding parallel to the fibers). When sliding in the axial direction, there are fewer obstacles (fibers) and therefore less resistance in pin movement, resulting in lower CoF. The dependence on speed may be attributed to the improved lubrication along the fibers versus across the fibers. At low speed this effect may not be perceptible as the fluid pressure does not build up, but it could gain in importance when the speed increases and the fluid remains trapped along the fibers rather than escaping laterally.

4.4. Limitations of the Current Study

4.4.1. Materials and Bone Structure

The current work investigated the effects of several parameters such as sliding speed, load, material and surface finish as well as the sliding direction on the friction properties of the bone-implant pair. Although these parameters are important in the evaluation of the friction of the bone-implant system, there are still some factors that shall be investigated further. Namely, the choice of 316 L steel instead of titanium alloys for many experiments can be questioned. The 316 L steel however represents historically the most common implant material and is still used in some countries and applications such as screws. Moreover, it is an industrial standard that can be reproduced by any laboratory.

Also, the bovine bone, used in our tribological experiments, has different microstructure than the human bone. The clinically relevant human bone microstructure is lamellar in comparison to the plexiform architecture of the bovine bone. Nevertheless, their elastic and post-yield properties are qualitatively similar and it is therefore expected that the observed trends in friction will remain valid but to be slightly different quantitatively.

4.4.2. Tribological conditions (linear motion, temperature, saline solution)

The tribological experiments were performed using linear reciprocating mode. Although the real path during the micromotions may be curvilinear and exhibit some hysteresis in vivo, we believe that the linear movement is a good approximation and can be most easily reproduced with industrial tribometers. We also acknowledge that the extent of the motion is larger in the experiment than in typical in vivo situations but a longer path is a constraint of common tribological systems. Using a nano-level system with shorter path control would not have offered the proper level of pressure. It is worth noting that all measurements were done at room temperature rather than at body temperature. Measurements at body temperature would be more realistic but it is well-known that the bulk material properties of bone are not highly sensitive to temperature. Accordingly, we did not expect significant changes in the tribological properties with temperature. Saline solution was used during our tests as it is the most common model for bone fluid. Since we already investigated numerous parameters, we did not explore the effects of different fluids. We do not know if proteins will have an influence in the presence of a rough bone surface, but this is certainly worth investigating in the future.

5. Conclusions

The present study investigated tribological properties of implant versus cortical bovine bone under various conditions. The effects of load, sliding speed, implant material, surface finish and direction of sliding were analyzed in a systematic tribological study which simulated real life conditions (walking and jumps) in the post-operation period. It was found that the CoF is affected more strongly by load than by sliding speed: a fifty-fold change in load resulted in similar change of CoF as a thousand-fold change in speed. At low speeds and loads (corresponding to walking) the CoF was found to be ~0.45 for 316 L steel and ~0.6 for the Ti and Ti-alloy implants. It was found that steel 316 L has generally lower coefficient of friction compared to the Ti and Ti alloy, which could be attributed to larger contact area and hence increase of CoF of these materials. The friction coefficient does not seem to be affected by the sliding direction; however at higher speeds a higher friction coefficient was observed when sliding in the circumferential direction than in the axial direction. Despite several limitations mentioned in the discussion, we believe that the presented results contribute to the understanding of the lubricated friction between bone and implant, which is crucial for modeling of this contact problem. The results will also help the development and optimization of new implants and their surface finish.

Acknowledgements

This research did not receive any specific grant from funding agencies in the public, commercial, or not-for-profit sectors, but the authors would like to acknowledge Nobel Biocare Services AG for

provision of the CP Ti material with surface treatment, and thank the workshop of ISTB for manufacturing the necessary parts. The advices of Marzieh Ovesy and the supervision of Benjamin Voumard in the laboratory are also gratefully acknowledged.

Appendix A

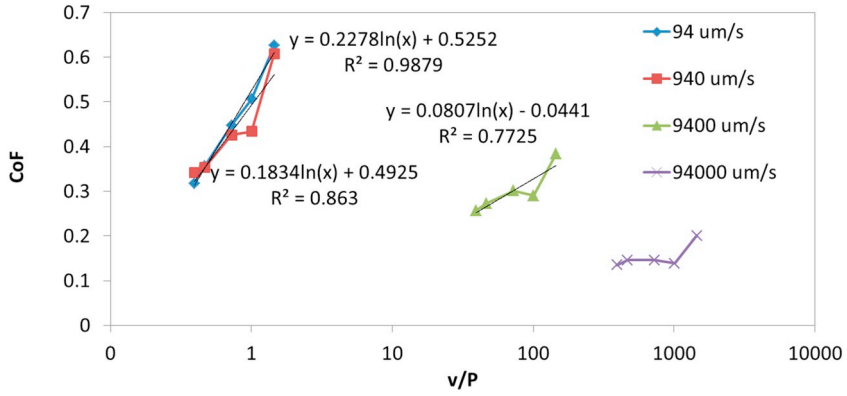

Fig. A1. Coefficient of friction as a function of sliding speed divided by load (v/P). To show the effect of the load, the data for each sliding speed were fitted (the slope of the fit is given in the chart). The higher the slope of the fit, the 'stronger' the effect of the load.

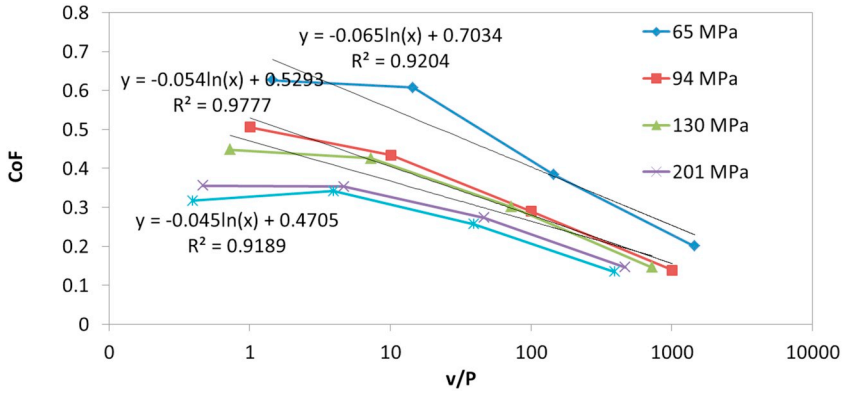

Fig. A2. Coefficient of friction as a function of sliding speed divided by load (v/P). To show the effect of the sliding speed, the data for each load were fitted (the slope of the fit is given in the chart). The higher the slope of the fit, the 'stronger' the effect of the speed. Note smaller (absolute) value of the slope of the speed fit compared to the slope of the load fit.

References

[1] D.f.d.l.D.O. fédéral de la statistique OFS, Communiqué de presse, Statistiques des établissements hospitaliers 2012: données provisoires, Un million de patients traités dans les établissements hospitaliers, (2013).

[2] T. Albrektsson, B. Albrektsson, Osseointegration of bone implants: a review of an alternative mode of fixation, Acta Orthop. Scand. 58 (1987) 567–577, https://doi.org/10.3109/17453678709146401.

[3] J. Ziebart, S. Fan, C. Schulze, P.W. Kämmerer, R. Bader, A. Jonitz-Heincke, Effects of interfacial micromotions on vitality and differentiation of human osteoblasts, Bone Joint Res. 7 (2018) 187–195, https://doi.org/10.1302/2046-3758.72.BJR-2017-0228.R1.

[4] R.M. Wazen, J.A. Currey, H. Guo, J.B. Brunski, J.A. Helms, A. Nanci, Micromotion-induced strain fields influence early stages of repair at bone–implant interfaces, Acta Biomater. 9 (2013) 6663–6674, https://doi.org/10.1016/j.actbio.2013.01.014.

[5] H.V. Oosterwyck, J. Duyck, J.V. Sloten, G.V. der Perre, M.D. Coomans, S. Lieven, R. Puers, L. Naert, The influence of bone mechanical properties and implant fixation upon bone loading around oral implants, Clin. Oral Implants Res. 9 (2001) 407–418, https://doi.org/10.1034/j.1600-0501.1996.090606.x.

[6] S. Thelen, F. Barthelat, L.C. Brinson, Mechanics considerations for microporous titanium as an orthopedic implant material, J. Biomed. Mater. Res. 69A (2004) 601–610, https://doi.org/10.1002/jbm.a.20100.

[7] T.M. Keaveny, E.F. Morgan, O.C. Yeh, Standard Handbook of Biomedical Engineering & Design: CHAPTER 8 BONE MECHANICS, in: Stand. Handb. Biomed. Eng. Des, McGRAW-HILL, New York, Chicago, San Francisco, Lisbon, London, Madrid, Mexico City, Milan, New Delhi, San Juan, Seoul, Singapore, Sydney, Toronto, 2003.

[8] M. Viceconti, R. Muccini, M. Bernakiewicz, M. Baleani, L. Cristofolini, Large-sliding contact elements accurately predict levels of bone–implant micromotion relevant to osseointegration, J. Biomech. 33 (2000) 1611–1618, https://doi.org/10.1016/S0021-9290(00)00140-8.

[9] J.E. Biemond, R. Aquarius, N. Verdonschot, P. Buma, Frictional and bone ingrowth properties of engineered surface topographies produced by electron beam technology, Arch. Orthop. Trauma Surg. 131 (2011) 711–718, https://doi.org/10.1007/s00402-010-1218-9.

[10] Y. Zhang, P.B. Ahn, D.C. Fitzpatrick, A.D. Heiner, R.A. Poggie, T.D. Brown, Original articles interfacial frictional behavior: cancellous bone, Crit. Bone 3 (1999) 245–251.

[11] M. Dammak, M. Schwartz, L. Gustavson, Friction properties at the bone – metal Interface : comparison of four different porous metal surfaces, J. Biomech. 35 (1997) 329–336.

[12] A. Hashemi, A. Shirazi-Adl, M. Dammak, Bidirectional friction study of cancellous bone-porous coated metal interface, J. Biomed. Mater. Res. 33 (1996) 257–267 (doi:10.1002/(SICI)1097-4636(199624)33:4 < 257::AID-JBM5 > 3.0.CO;2-O).

[13] N.B. Damm, M.M. Morlock, N.E. Bishop, Friction coefficient and effective interference at the implant-bone interface, J. Biomech. 48 (2015) 3517–3521, https://doi.org/10.1016/j.jbiomech.2015.07.012.

[14] J.A. Grant, N.E. Bishop, N. Götzen, C. Sprecher, M. Honl, M.M. Morlock, Artificial composite bone as a model of human trabecular bone: the implant-bone interface, J. Biomech. 40 (2007) 1158–1164, https://doi.org/10.1016/j.jbiomech.2006.04.007.

[15] H.Y.Z.B. Yu, Z.R. Cai, M.H. Zhu, Fretting behavior of cortical bone against titanium and its alloy, Wear 259 (2005) 910–918, https://doi.org/10.1016/j.wear.2005.01.037.

[16] X. Yangtao, Y. Yan, X. Tiandong, Study on fretting friction coefficient between NiTi shape memory alloy and human bone in Hank's solution, Rare Metal Mater. Eng. 37 (2008) 1201–1205, https://doi.org/10.1016/S1875-5372(09)60032-1.

[17] M.J. Mirzaali, A. Bürki, J. Schwiedrzik, P.K. Zysset, U. Wolfram, Continuum damage interactions between tension and compression in osteonal bone, J. Mech. Behav. Biomed. Mater. 49 (2015) 355–369, https://doi.org/10.1016/j.jmbbm.2015.05.007.

[18] R.G. Budynas, J.K. Nisbett, J.E. Shigley, Shigley's Mechanical Engineering Design, Tenth edition, McGraw-Hill Education, New York, NY, 2015.
[19] M.A. Chowdhury, M.K. Khalil, D.M. Nuruzzaman, M.L. Rahaman, The effect of sliding speed and normal load on friction and wear property of aluminum, Int. J. Mech. Eng. 11 (2011) 53–57 (10.1.1.369.1903).
[20] J. Williams, Engineering Tribology, Cambridge University Press, 1994.
[21] J.P. Davim, Biomaterials and Medical Tribology: Research and Development, Elsevier, 2013.
[22] C. Wang, G. Zhang, Z. Li, X. Zeng, Y. Xu, S. Zhao, H. Hu, Y. Zhang, T. Ren, Tribological behavior of Ti-6Al-4V against cortical bone in different biolubricants, J. Mech. Behav. Biomed. Mater. 29 (2018), https://doi.org/10.1016/j.jmbbm.2018.10.031.